Fluorescence Decays and Spectral Properties of Rhodamine B in Submono-, Mono-, and Multilayer Systems

5 AUTHORS, INCLUDING:

Klaus Kemnitz
EuroPhoton GmbH
61 PUBLICATIONS   1,844 CITATIONS

SEE PROFILE

Naoto Tamai
Baiko Jo Gakuin University
188 PUBLICATIONS   5,928 CITATIONS

SEE PROFILE

Nobuaki Nakashima
Toyota Physical and Chemical Institute
214 PUBLICATIONS   4,358 CITATIONS

SEE PROFILE

Keitaro Yoshihara
The Graduate University for Advanced Studies
303 PUBLICATIONS   8,231 CITATIONS

SEE PROFILE

Fluorescence Decays and Spectral Properties of Rhodamine B in Submono-, Mono-, and Multilayer Systems

Klaus Kemnitz,[†] Naoto Tamai, Iwao Yamazaki, Nobuaki Nakashima, and Keitaro Yoshihara*

Institute for Molecular Science, Myodaiji, Okazaki 444, Japan (Received: February 21, 1986; In Final Form: May 23, 1986)

Absorption and fluorescence properties of rhodamine B in submono-, mono- and multilayer systems adsorbed on fused quartz plates have been studied at 295 and 77 K. Existence of fluorescent and nonfluorescent dimers of rhodamine B at 295 K and a structural change of the aggregate geometry at low temperatures have been postulated. Rates of nonradiative decay and photoinduced electron transfer of dimers adsorbed on organic crystals and their possible role in hole injection are discussed.

I. Introduction

In studying the coverage dependence of the fluorescence dynamics of rhodamine B (RhB) adsorbed on glass and naphthalene,[1] we observed a nonexponential decay caused by two-dimensional Förster-type energy transfer from the excited RhB monomer to the dimer species[2] together with an additional exponential component. This fast exponential decay, whose contribution increased with surface coverage, was interpreted as the fluorescence of two-dimensional RhB dimers. Dimer fluorescence of RhB was not observed at ambient temperature before (e.g. in solution), though hints for the existence of a RhB species with red-shifted fluorescence were obtained by the observation of its amplified emission.[3] Dimer fluorescence spectra and decays were obtained, however, at 77 K in a matrix.[4] We tried to observe the dimer fluorescence at 295 K in highly concentrated aqueous solution but failed in spite of optimization of excitation and observation wavelengths and employing a very sensitive detection system. Dimer fluorescence in solution at 295 K is supposed to be very weak and obscured by the dominant monomer fluorescence. Adsorption, however, suppresses nonradiative transitions induced by intramolecular reorientation and by diffusional collision with solvent molecules and thus enhances the radiative processes. For example, phosphorescence can be observed at 295 K from adsorbed molecules which do not phosphoresce in solution.[5] This paper further investigates the properties of fluorescent and nonfluorescent dimers of RhB adsorbed on a surface. Evidence for the existence of fluorescent dimers at room temperature and for the fluorescence of higher aggregate species at 77 K were obtained from absorption and fluorescence spectra and fluorescence dynamics.

The present paper is organized in the following way: after the Experimental Section, we briefly, review in section III the standard theory of exciton singlet splitting in order to familiarize the reader with the existence of RhB dimers of fluorescent geometries which may be encountered in the adsorbed state. In the first part of section IV we try to characterize the adsorption sites of RhB on glass by estimating their polarity from the observed solvent shift, and in the following parts, we present our spectral and temporal data obtained for mono- and multilayer systems from which we deduced the existence of several emitting species of RhB in the adsorbed state. In the final part of section IV we discuss the hole injection capabilities of RhB dimers and aggregates in view of the existence of fluorescent RhB dimers.

II. Experimental Section

The fluorescence decays of RhB were measured with a time-correlated single-photon-counting system with subnanosecond time resolution, which has been described elsewhere.[6] Here we confine ourselves to an outline of the light source. The picosecond laser system was composed of a synchronously pumped, cavity dumped dye laser (Spectra Physics 375 and 344 S) and a mode-locked argon ion laser (Spectra Physics 171-18). The dye laser was operated at a repetition rate of 800 kHz, the time duration of a single pulse being 6 ps (fwhm). The average power of the dye laser was adjusted to 7×10^{-4} W/cm^2 which corresponds to 10^8 photons/cm^2 per single pulse at 570 nm. The photomultiplier employed was a Hamamatsu microchannel plate version (R 1294U) which gave an observed laser pulse width as short as 70 ps (fwhm).[6] This type of microchannel plate photomultiplier has a temporal response function which is independent of the wavelength.[7]

Fluorescence was collected at right angles to the excitation beam. The quartz plates with the adsorbed layer were aligned at an angle of about 55° to avoid reflection of the exciting light into the slit of the monochromator. An appropriate number of cutoff filters were used to reject all scattered and reflected excitation light. The fluorescence measurements were performed under argon atmosphere using an optical dewar. All samples were flushed with argon for 15 min to displace adsorbed oxygen. This procedure prevented photoreactions of the adsorbed dye which are observed if the sample is exposed to prolonged irradiation at ambient conditions.[8]

RhB was from Katayama Chemicals and recrystallized before use. The purity was greater than 95% as determined by absorbance measurement and TLC.[9] To further assess the purity, we measured the fluorescence decay of a 10^{-6} M aqueous solution, which had a strictly single exponential decay of lifetime $\tau = 1.63$ ns, observed at the magic angle and $\lambda_{obsd} = 575$ nm. Monolayers of RhB were produced by adsorption from a 10^{-4} M aqueous solution,[10] submonolayers by adsorption from increasingly diluted solutions, and multilayers by vacuum deposition. Adsorption from aqueous solution was completed in about 10 min, the residual dye solution was then removed by soaking it off with a tissue paper.[11] Suprasil quartz plates which were sonicated successively in Decon

(1) Kemnitz, K.; Murao, T.; Yamazaki, I.; Nakashima, N.; Yoshihara, K. *Chem. Phys. Lett.* **1983**, *101*, 337.

(2) Nakashima, N.; Yoshihara, K.; Willig, F. *J. Chem. Phys.* **1980**, *73*, 3553.

(3) Chin, S. L. *Phys. Lett.* **1974**, *48A*, 403.

(4) Chambers, R. W.; Kajiwara, T.; Kearns, D. R. *J. Phys. Chem.* **1974**, *78*, 380.

(5) Schulman, E. M.; Walling, C. *J. Phys. Chem.* **1973**, *77*, 902.

(6) Murao, T.; Yamazaki, I.; Yoshihara, K. *Appl. Opt.* **1982**, *21*, 2297.

(7) Demas, J. N. *Excited State Lifetime Measurements*; Academic Press: New York, 1983.

(8) Liang, Y.; Moy, P. F.; Poole, J. A.; Ponte Goncalves, A. M. *J. Phys. Chem.* **1984**, *88*, 2451.

(9) Horobin, R. W.; Murgatroyd, L. B. *Stain Technol.* **1969**, *44*, 297.

(10) Gerischer, H.; Willig, F. *Topics in Current Chemistry*, Boschke, F. L., Ed.; Springer: Berlin, 1976.

(11) It has to be noted here that several other techniques for dye (mono)layer preparation are in use, e.g., the spinning[12] and the dipping technique.[13] A comparison of results obtained from layer systems prepared according to these techniques may not always be possible, therefore.

(12) Heinz, T. F.; Chen, C. K.; Ricard, D.; Shen, Y. R. *Phys. Rev. Lett.* **1982**, *48*, 478.

(13) Garoff, S.; Stephens, R. B.; Hanson, C. D.; Sorenson, G. K. *Opt. Commun.* **1982**, *41*, 257.

[†] Present address: Department of Chemistry, Columbia University, New York, NY 10027.
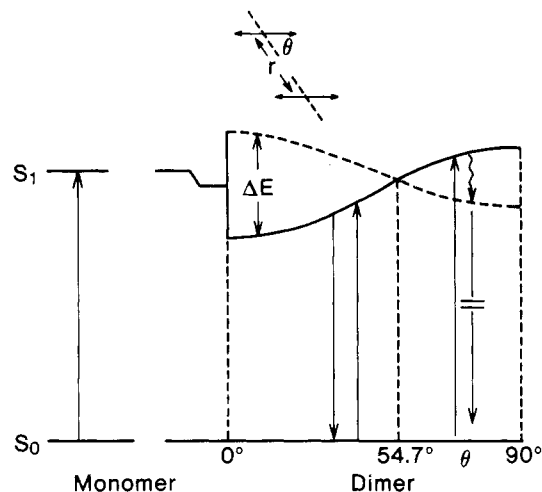
Type	Exciton Splitting	Spectral Properties	Geometry
(1)	$4\left(\frac{N-1}{N}\right)\left(\frac{\mu^2}{r^3}\right)(1-3\cos^2\theta)$	fluorescent or nonfluorescent red or blue shift of absorption	
(2)	$2\left(\frac{\mu^2}{r^3}\right)$	nonfluorescent blue shift of absorption	
(3)	$4\left(\frac{\mu^2}{r^3}\right)$	fluorescent red shift of absorption	
(4)	$16\left(\frac{\mu^2}{r^3}\right)$	fluorescent red shift of absorption	
(5)	$2\left(\frac{\mu^2}{r^3}\right)(1+\cos^2\theta)$	fluorescent red and blue shift of absorption	

Figure 1. Exciton singlet splitting for dimers with in-plane transition moments of varying angle of inclination θ.[19] Also included is the formula of splitting for a two-dimensional array and for a dimer of nonparallel transition moments.

90, acetone, and distilled water before adsorption of the dye served as substrates for these layer systems. The coverage was determined optically by measuring the absorbance and, for multilayer systems, was additionally monitored and determined by a Sloan thickness meter (DMT 200).

The fluorescence spectra were recorded with a Shimadzu fluorospectrophotometer RF-502. The absorption spectra at lower coverages were obtained with a highly sensitive spectrophotometer based on the single-photon-counting technique[14] and at higher coverages with a Hitachi 556 spectrophotometer where several dye layers were stacked together. Measurements at 77 K were performed by immersing the sample in liquid nitrogen using an optical dewar.

III. Dimer Geometry and the Theory of Exciton Splitting

Throughout the literature of the past 20 years, it was constantly assumed that dimers of RhB and related dyes are generally nonfluorescent.[15,16] This is certainly true for dimers dissolved in low viscosity solvents like water at room temperature. Adsorption, however, can drastically alter geometry and thus spectral and temporal properties of dimer fluorescence. By briefly reviewing results obtained from the simple exciton model for various aggregate geometries, we demonstrate that the fluorescent character of any dimer is exclusively determined by the mutual orientation of its monomeric constituents. The nonfluorescent (or weakly fluorescent) sandwich-type dimer of RhB in aqueous solution is merely one special case. On a surface with its various adsorption sites, a whole spectrum of fluorescent and nonfluorescent in-plane two-dimensional dimers may exist, however.

(14) Yamamoto, N.; Sawada, T.; Tsubomura, H. *Bull. Chem. Soc. Jpn.* **1979**, *52*, 987.

(15) Itoh, K.; Chiyokawa, Y.; Nakao, M.; Honda, K. *J. Am. Chem. Soc.* **1984**, *106*, 1620.

(16) Avnir, D.; Levy, D.; Reisfeld, R. *J. Phys. Chem.* **1984**, *88*, 5956.

TABLE I: Observed and Calculated Spectral Shifts of Absorption Spectra[a]

solvent	n^2	D	$\Delta\bar{\nu}$, cm^{-1} calcd	$\Delta\bar{\nu}$, cm^{-1} obsd	λ_{max} (obsd), nm	ref
vapor	1	1	0	0	450	27
DMA	2.06	38.9	4164	4333	559	28
EtOH	1.85	24.6	3930	3806	543	29
water	1.78	78.5	4154	4172	554	
n-BuOH	1.95	17.5	3836	3840	544	30
glycerol	2.17	42.5	4232	4236	556	30
MeOH	1.76	32.7	3972	3907	546	31
bonded to PMA					563	30
adsorbed on glass	2.13	4	2715	4301	558	

[a] $M_{00} = 25$ D,[25] $M_{ii} - M_{00} = 1.7$ D,[26] $L = 1000$ Å, $a = 5$ Å,[24] DMA = N,N-dimethylacetamide, PMA = poly(methacrylic acid).

Figure 1 summarizes the results for in-plane dimers and aggregates as obtained from the theory of exciton splitting.[17-19] The diagram shows the exciton splitting (ΔE) for dimers with in-plane, parallel transition moments as a function of the angle of inclination θ, which is the angle of the monomer transition moments with the connecting lines of the monomer centers. Formulas 1–5 in Figure 1 give the energy splitting of the singlet levels for different geometries, where N represents the number of monomer molecules forming the aggregate, r the center-to-center distance of monomers, and μ the monomer transition moment. The splitting is zero at the magic angle of 54.7° but nonzero for larger and smaller angles. The selection rules for radiative transition are different on both sides of this angle. For angles smaller than 54.7°, the transition to the lower singlet level is allowed and the species are fluorescent; for angles larger than 54.7°, the transition is allowed to the upper singlet level and fluorescence, which could occur from the lower singlet level after fast internal conversion, is forbidden. We can see that a variety of both fluorescent and nonfluorescent dimers could coexist on a surface, the only criterion for fluorescent or nonfluorescent character being simply the angle θ.

Formula 1 in Figure 1 describes the angular dependence of the singlet spitting in general (diagram). Formula 2 represents dimers of sandwich-type structure with $\theta = 90°$ and depicts the weakly fluorescent dimer in solution.[20] Formula 3 stands for a fluorescent head-to-tail species as it might exist in the adsorbed state and formula 4 shows the large splitting which results for a two-dimensional lattice-like array of wide extension. Common to all cases described so far are co-planar, parallel transition moments. This situation results in selection rules where the transition is allowed to either the lower or the upper singlet level, which causes a red or a blue shift of the absorption maximum. For alignments of the transition moments other than described above, transitions can be allowed to both levels and a red and blue shift (splitting) is observed, for example, dimers of type 5 in Figure 1. For the latter geometry, the radiative lifetime depends on the angle θ.[17] The above simple model of exciton splitting neglects vibrational interaction[21] of both monomer moieties but has the advantage of simplicity and power of illustration and may suffice for the above qualitative considerations.

IV. Results and Discussion

1. Absorption and Fluorescence Spectra. a. Solvent Effect and Polarity of Adsorption Sites. Figure 2 shows the dependence on the coverage of the absorption and fluorescence spectra of RhB. The spectra in the adsorbed state (solid lines) are compared with the solution spectra of RhB monomers at low concentration (broken lines). The vertical solid lines indicate the vibrational structure of the monomer species.

(17) McRae, E. G.; Kasha, M. *J. Chem. Phys.* **1958**, *28*, 721.

(18) Hochstrasser, R. M.; Kasha, M. *Photochem. Photobiol.* **1964**, *3*, 317.

(19) Kasha, M.; Rawls, H. R.; El-Bayoumi, M. A. *Pure Appl. Chem.* **1965**, *11*, 371.

(20) Gal, M. E.; Kelly, G. R.; Kurucsev, T. *J. Chem. Soc., Faraday Trans. 2* **1973**, *69*, 395.

(21) Fulton, R. L.; Gouterman, M. *J. Chem. Phys.* **1964**, *41*, 2280.
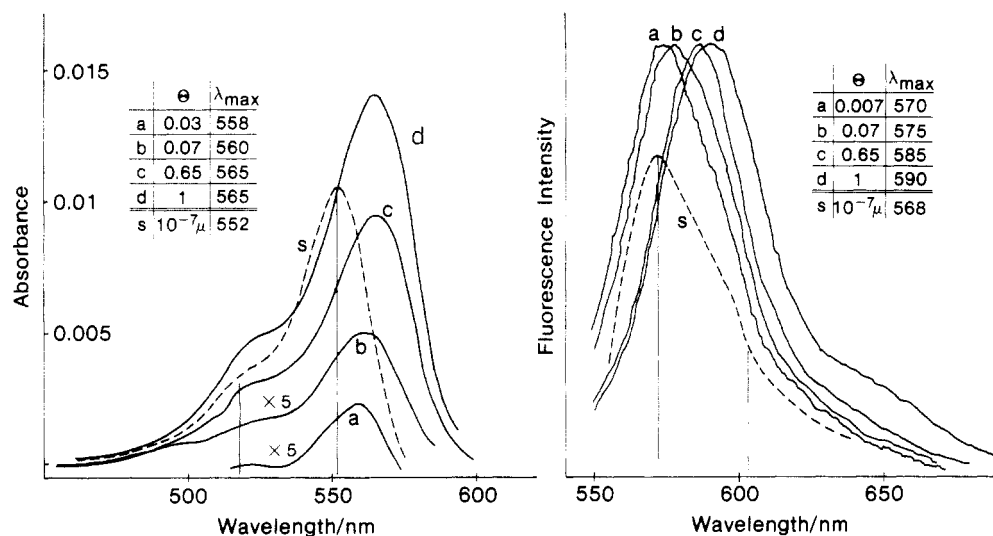
Figure 2. Coverage dependence of the absorption and fluorescence spectra of RhB adsorbed on fused quartz plates. The coverage (Θ) increases from a to d; $\Theta = 1$ corresponds to a monolayer. S stands for dilute aqueous solution of 10^{-7} M. Vertical lines indicate the vibrational progression of the monomer species. The coverage of the absorption spectra were calculated with $\epsilon = 1.1 \times 10^5$ M^{-1} cm^{-1} and an area per molecule of 150 Å^2. The fluorescence spectra are uncorrected, the excitation wavelength being 530 nm.

Monomeric adsorption from diluted aqueous solution onto glass causes a small red shift of the absorption maximum and almost no red shift of the fluorescence maximum (s → a, Figure 2). No shift was observed by Mulder[22] for the absorption maximum (action spectrum) of RhB adsorbed on crystals of anthracene and by Spitler and Calvin[23] for the adsorption of RhB on ZnO at submonolayer coverages. To assess these surprisingly small spectral shifts and the environmental conditions of adsorbed molecules of RhB, we tabulated the spectral shift of the absorption maximum of RhB monomers adsorbed on glass together with reported values for solutions of RhB in various solvents and for the vapor phase. Table I includes dielectric constant D and refractive index n of the solvents and the calculated red shift of absorption maxima relative to the vapor, using McRae's formula:[24]

$$\Delta\bar{\nu} = (AL + B)(n^2 - 1)/(2n^2 + 1) +$$
$$C\{(D - 1)/(D + 2) - (n^2 - 1)/(n^2 + 2)\} \quad (1)$$

where A, B, and C are properties of the solute and L is the "weighted mean wavelength". A and B are related to the dispersion force interactions of the solute with the solvent and $C = (2/hc)M_{00}(M_{00} - M_{ii})/a^3$. C is calculated from the experimental dipole moments M_{00} and M_{ii} for the ground and excited singlet state of RhB and an estimated cavity radius a (see Table I). A plot of $\Delta\bar{\nu}$(calcd) vs. $\Delta\bar{\nu}$(obsd) yields a good correlation and is shown in Figure 3. Best fit is obtained for $A = 4.5 \times 10^8$ cm^{-2} and $B = -4500$ cm^{-1} which is close to the experimental values obtained for the dye phenol blue.[24] The points are fitted to the straight line with a root mean square deviation of 65 cm^{-1} (≈ 2 nm).

McRae's formula (eq 1), which was used to calculate the solvent shift of the absorption maximum, does not consider effects due to hydrogen bonding. The good correlation of calculated and observed red shifts for solvents with varying H-donating power can be taken, therefore, as a hint that hydrogen bonds to the
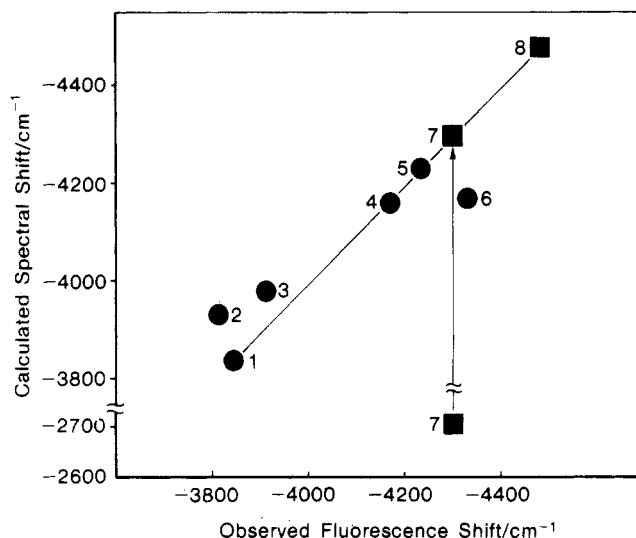

Figure 3. Correlation of observed and calculated absorption red shifts of Table I according to eq 1. Circles indicate solvents: 1, butanol; 2, ethanol; 3, methanol; 4, water; 5, glycerol; and 6, N,N-dimethylacetamide. Squares indicate dye adsorbed or bonded on surfaces: 7, adsorbed on fused quartz glass; 8, bonded to PMA. The arrow indicates the shift from $D = 4$ to $D_{eff} = 70$ to correlate data for RhB adsorbed on glass.

dissolved molecule are negligible. This is not surprising, since all main hydrogen acceptors, i.e., the two nitrogen and the oxygen atom in the xanthene skeleton, carry a partial positive charge.[32] H bonds to the carboxyl group do not influence the absorption properties to a large degree because of the perpendicular aligment of the carboxylphenyl group with respect to the xanthene chromophore.[29] Figure 3 also shows the observed shift for RhB adsorbed on glass which is much larger than the calculated value (Table I). This shift was computed, however, from the bulk dielectric constants of glass. The static dielectric constant D on the surface is certainly much larger than the bulk value, due to the polar siloxane and silanol groups of a glass surface[33] and coadsorbed water molecules. In order to obtain a correlation with the other solvents, an efficient D of about 70 has to be assumed. Included in Figure 3 is the large red shift of RhB bonded to poly(methacrylic acid) (PMA) which is even larger than that of

(22) Mulder, B. J. *Philips Res. Rep.* **1967**, *22*, 553.
(23) Spitler, M.; Calvin, M. *J. Chem. Phys.* **1977**, *67*, 5193.
(24) McRae, E. G. *J. Phys. Chem.* **1957**, *61*, 562.
(25) Stevens, B.; Connelly, N.; Suppan, P. *Spectrochim. Acta* **1966**, *22*, 2121.
(26) Schmidt, S.; Reich, R. *Ber. Bunsenges. Phys. Chem.* **1972**, *76*, 599.
(27) Pappalardo, R.; Ahmed, S. *J. Chem. Phys.* **1972**, *56*, 5135.
(28) Hirano, K. *Nippon Kagaku Kaishi* **1974**, *10*, 1823.
(29) Drexhage, K. H. *Topics in Applied Physics*, Vol. 1, Schäfer, F. P., Ed.; Springer: Berlin, 1973; p 144.
(30) Snare, M. J.; Tan, K. L.; Treloar, F. E. *J. Macromol. Sci. Chem.* **1982**, *A17*, 189.
(31) Seki, H.; Itoh, U. *Rev. Sci. Instrum.* **1980**, *51*, 22.

(32) Pilipenko, A. T.; Savransky, L. I.; Shin, Nguen Mong *Zh. Anal. Khim.* **1969**, *24*, 460.
(33) Snyder, L. R. *J. Phys. Chem.* **1963**, *67*, 2622.

water. Snare et al.[30] suggested a binding site which is more polar than water itself and envisioned a carboxylic acid group to which the RhB molecule is bonded. The high polarity of adsorption sites on glass was also postulated by Nakashima and Phillips[34] who studied 1,1'-bianthryl adsorbed on porous Vycor glass. Another probe for the polarity of adsorption sites is pyrene, which is increasingly used to investigate microenvironments.[35,36] Observation of the vibrational structure of the fluorescence spectrum of pyrene showed the same ratio of the intensities of the first and third peak when dissolved in water or adsorbed on glass. Rhodamine 6G (Rh6G) embedded in a matrix of silica gel glass[16] may serve as a further example, demonstrating the polarity of glass surfaces. Our estimation of $D_{eff} \approx 70$ (using $n = 1.43$) suggests a binding site which is very similar to water. $D_{eff} \approx 70$ is a very crude estimation; however, it is sensitive to the reflective index used and to λ_{max}.

b. Coverage Dependence. A more pronounced effect on the absorption and emission spectra is observed when the coverage is successively increased from $1/100$ to a full monolayer (a $\rightarrow$ d, Figure 2). An identical red shift of the absorption maximum was observed by Spitler and Calvin[23] for the adsorption of RhB on single crystals of ZnO and earlier, more qualitatively, by Mulder,[22] who observed a red shift for the action spectrum of RhB adsorbed on anthracene crystals upon increasing the coverage. Recently, a red shift for both absorption and fluorescence maxima of Rh6G adsorbed on glass was reported by Garoff et al.,[13] analogous to that of RhB described in this work.

To explain the observed red shift, Mulder assumed interaction of the dye monomer with neighboring molecules and suggested "in-plane associates" of dye molecules.[22] We used the "simple" molecular exciton model which has been formulated in the previous section for dimers, aggregates, and lattice-like arrangements of various geometries[17-19] to explain the experimental red shifts of $650-1850$ cm^{-1} (Figure 2 and 4) for monolayer and multilayers and also to deduce possible geometries of the in-plane dimers and their spectral properties.

Figure 2 shows that the red shift of the fluorescence maximum is about twice the red shift of the absorption maximum. This turns out to be a very significant observation inasmuch as it is leading to a picture of variable dimer geometry. We imagine a surface comprised of a variety of adsorption sites where many different dimer species could coexist. Species of type 1 (Figure 1, for $\theta < 55°$) would contribute to the red shift of both fluorescence and absorption spectra; species of type 1 for $\theta > 55°$ would contribute to the red shift of fluorescence and to a blue shift of absorption. All species on the surface contribute to the red shift of fluorescence, but only a portion of them would contribute to the red shift of absorption. Consequently, we observe a large red shift of the fluorescence maximum, a smaller red shift of the absorption maximum, and an increase of the intensity of the shoulder (corresponding to a blue shift) at the shorter wavelength side of the absorption maximum (Figure 2, the position of the monomer vibrational shoulder coincides with the short wavelength maximum of the dimer[4]). The superposition of the absorption spectra of a variety of fluorescent and nonfluorescent or weakly fluorescent dimer species together with the residual monomers, creates an overall appearance which resembles the monomer absorption spectrum. This may explain why dimer fluorescence could evade detection so far, since the absence of a solution dimer-like absorption or action spectrum was taken as criterion for the absence of dimer in the adsorbed state.

An alternative explanation for fluorescence and absorption red shifts could be seen in the increasing polarity of the surface with increasing dye coverage, since RhB is adsorbed as a zwitterion.[37] This solvent polarity effect would shift fluorescence and absorption spectra of the monomer species to the red.[38]   However, this

(34) Nakashima, N.; Phillips, D. *Chem. Phys. Lett.* **1983**, *97*, 337.
(35) Levitz, P.; Van Damme, H.; Keravis, D. *J. Phys. Chem.* **1984**, *88*, 2228.
(36) Kalyanasundaram, K.; Thomas, J. K. *J. Am. Chem. Soc.* **1977**, *99*, 2039.
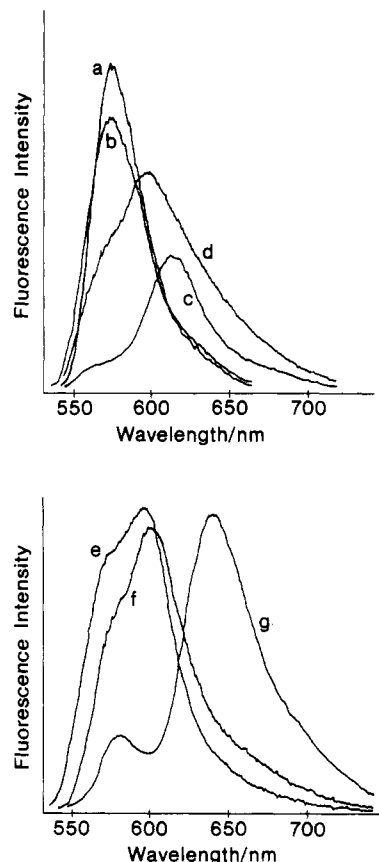(37) Ramette, R. W.; Sandell, E. B. *J. Am. Chem. Soc.* **1956**, *78*, 4872.

Figure 4. Temperature dependence of the fluorescence spectra of submono- and monolayer (top)[39] and multilayers of RhB (bottom) adsorbed on fused quartz plates. a and b represent the fluorescence spectra of a submonolayer at 77 and 295 K, respectively, both fluorescence peaks are at 573 nm. c and d are the fluorescence spectra of a monolayer at 77 and 295 K, respectively, with the fluorescence peaks at 623 and 595 nm. e and f are the fluorescence spectra of a multilayer system at 295 K before and after cooling to 77 K (peak at 600 nm for e), and g is the corresponding spectrum at 77 K (maxima at 580 and 640 nm). All spectra are uncorrected; the excitation wavelength was 530 nm. The scale of the intensity of the monolayer fluorescence at 77 K is reduced by approximately a factor of ten. Note that spectra c to g show the monomer shoulder (peak) at the short wavelength side of the maximum.

possibility can be excluded since at low temperatures the monomeric fluorescence peak always appears at 573–580 nm in submono-, mono-, and multilayer systems (Figure 4) and seems to be independent of the number of neighboring molecules. Apart from this observation, the fluorescence intensity at longer wavelengths increased drastically at low temperature (vide infra) and is in good accord with the observation of dimers in solution.[4]

c. Temperature Dependence. Figure 4 shows the temperature dependence of the fluorescence spectra of RhB in submono-, mono-, and multilayers. Figure 4 (top) compares the spectral change of the submonolayer and monolayer on lowering the temperature. The submonolayer spectrum is sharper at 77 K (a), but retains its maximum at about 573 nm. In contrast, the monolayer spectrum at 77 K (c) is clearly different from the spectrum at 295 K. The maximum is shifted from 595 to 623 nm and the shift is accompanied by an increase in fluorescence intensity of about 10 times (not scaled in the figure). The corresponding red shift in the multilayer system is even more pronounced (Figure 4, bottom). The spectral change is reversible (partially) as seen in Figure 4 (bottom) for the sequence e $\rightarrow$ g $\rightarrow$ f. Figure 4 reveals the presence of four emitting species with maxima at 573, 595, 623, and 640 nm. Species I with the observed fluorescence maximum in the range of 573–580 nm, present in submonolayer systems at 295 and 77 K, is easily identified as the monomer (see also Figure 2, ref 39). Species II with the max-

(38) Mataga, N.; Kubota, T. *Molecular Interaction and Electronic Spectra*; Marcel-Dekker: New York, 1970.
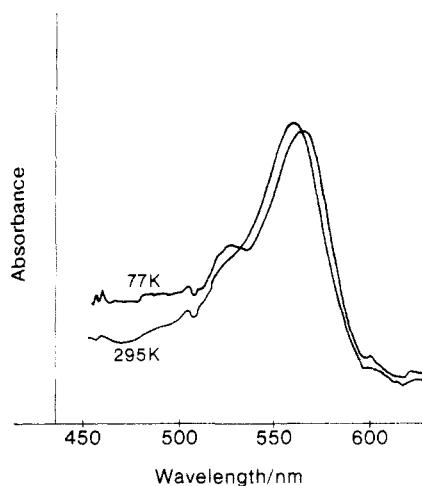
Figure 5. Temperature dependence of the absorption spectrum of a RhB monolayer adsorbed on a quartz plate. The absorption maximum at 295 K is located at 562 nm which shifts to 566 nm at 77 K. The short wavelength shoulder seen at 295 K develops into a peak at 77 K (528 nm).

imum at 590–600 nm is identified as a dimer occurring in mono- and multilayer at room temperature (see also Figure 2). Species III and IV with red-shifted maxima at 623 and 640 nm are two distinct dimers or aggregates present and emitting at 77 K. These large red shifts of species III and IV will be connected to a change of aggregation occurring at low temperatures. It should be noted that our monolayer systems are predominantly composed of dimers (Figures 2 and 4, in the latter, the presence of monomers is indicated as a shoulder at the short wavelength side of the dimer peak). This observation will be of importance for the discussion of monomer–monomer vs. dimer–dimer energy migration (see section IV2d).

Figure 5 shows the temperature dependence of the absorption spectra of a monolayer system. The changes in the absorption spectrum upon lowering the temperature consist of a small red shift of the absorption maximum and of an increase of the shoulder at about 528 nm. It is accompanied by a fluorescence red shift analogous to that in Figure 4 (top). If we tentatively assume that this fluorescent species at 77 K is a dimer of type 5 in Figure 1 with allowed transitions to both singlet levels, then we calculate a splitting of the singlet levels (from the absorption spectrum) of about 1270 cm^{-1}. On the other hand, the analogous splitting calculated from the shift of the fluorescence maximum would be about 2800 cm^{-1}. This apparent discrepancy between both calculated singlet splittings could be either attributed to neglecting the effect of vibronic coupling as it was demonstrated for the example of the sandwich dimer in solution[4] or to the overlap of spectra of a multitude of emitting and nonemitting species.

The observed change of the absorption spectrum (Figure 5), along with the large red shift of fluorescence (Figure 4) and the about tenfold increase of fluorescence intensity (accompanied by an increase of fluorescence lifetime, vide infra) upon lowering the temperature to 77 K, seems to indicate a structural change in the aggregational state.

To assess the magnitude of observed fluorescence red shifts,[40] we show in Figure 6 four models of two-dimensional RhB dimers
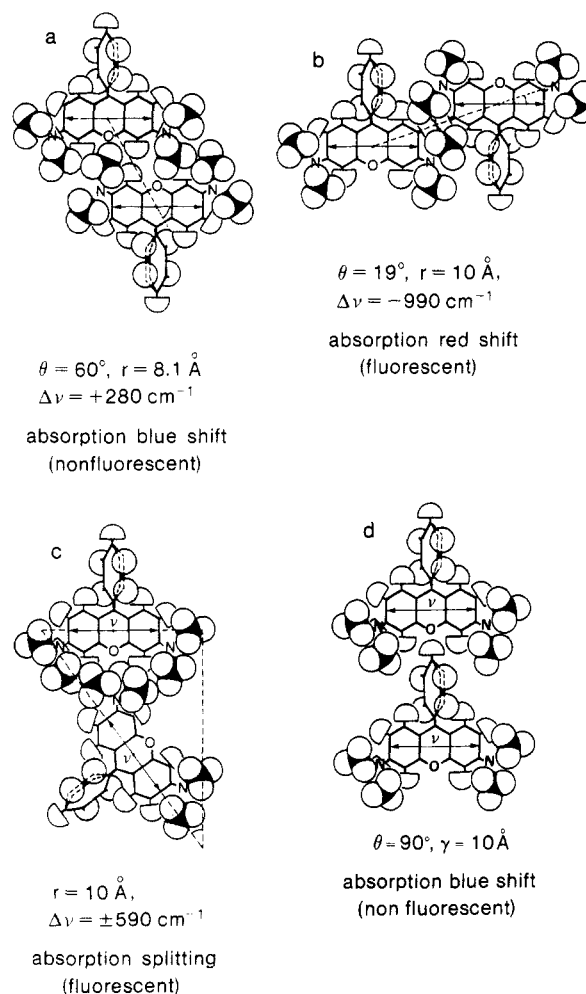

Figure 6. Model calculations[42] of spectral shifts for in-plane RhB dimers of varying geometry. Also indicated is their fluorescence character. Species a and b represent the nonfluorescent and fluorescent variant of dimers with in-plane, parallel transition moments ((1) in Figure 1), species c represents dimers with nonparallel alignment ((5) in Figure 1), and species d exemplifies a dimer structure whose geometry is determined by the electrostatic interaction of the RhB zwitterions.

and their calculated shifts. In comparison, the observed fluorescence red shifts are as follows:

$$\Delta\nu(\text{monolayer, 295 K}) = 645 \text{ cm}^{-1}$$

$$\Delta\nu(\text{monolayer, 77 K}) = 1400 \text{ cm}^{-1}$$

$$\Delta\nu(\text{multilayer, 295 K}) = 785 \text{ cm}^{-1}$$

$$\Delta\nu(\text{multilayer, 77 K}) = 1830 \text{ cm}^{-1}$$

$$\Delta\nu(\text{solution, 77 K}) = 1200 \text{ cm}^{-1} \text{ (ref 4)}$$

The calculations in Figure 6 were performed by using the transition moment $\mu^2 = 1.17 \times 10^{-34}$ esu^2 cm^2,[41] typically for fully allowed transitions. The model considerations in Figure 6 indicate that the maximal possible shift of in-plane dimers is about 1000 cm^{-1} (according to the simple exciton model), thus much smaller than correspondingly calculated shifts for three-dimensional sandwich-like species. This reflects the larger distance r of closest approach in the two-dimensional case. The observed fluorescence shifts for mono- and multilayers at 77 K (1400–1830 cm^{-1}) appear

---

(39) The fluorescence spectrum in Figure 4 for the monolayer at 295 K is slightly different from the monolayer spectrum in Figure 2. This reflects the inhomogeneity of the surface of glass where different monomer/dimer ratios can occur, varying from spot to spot, and from sample to sample, as was also observed by Liang et al.[8] Therefore, by measuring many spots on many different samples, representative spectra for a given coverage are obtained (Figure 2). It turned out that for a monolayer, the spectra always showed more dimer than monomer species (Figures 2 and 4).

(40) The fluorescence red shifts are not influenced by reabsorption which can be excluded because of the weak absorbance of both monolayer and 50-Å film. The absorbance of a 50-Å film corresponds to that of a 2 × 10^{-7} M solution in a 1-cm cell which is far below the onset of reabsorption effects which were found to occur for aqueous solutions with concentrations larger than 10^{-6} M.

(41) Turro, N. J. *Modern Molecular Photochemistry*; Benjamin/Cummings: London, 1978.

(42) Calculations were performed with the simple exciton model. All values are obtained for the point dipole approximation which results in overestimated splittings at small separations of monomers.[43] This does not, however, influence our conclusions which are of comparative character, since our calculated $\bar{\nu}_{\text{max}} \leq 1000$ cm^{-1} for in-plane dimers would even be somewhat smaller using the extended dipole approximation.

(43) Czikklely, V.; Forsterling, H. D.; Kuhn, H. *Chem. Phys. Lett.* **1970**, *6*, 207.
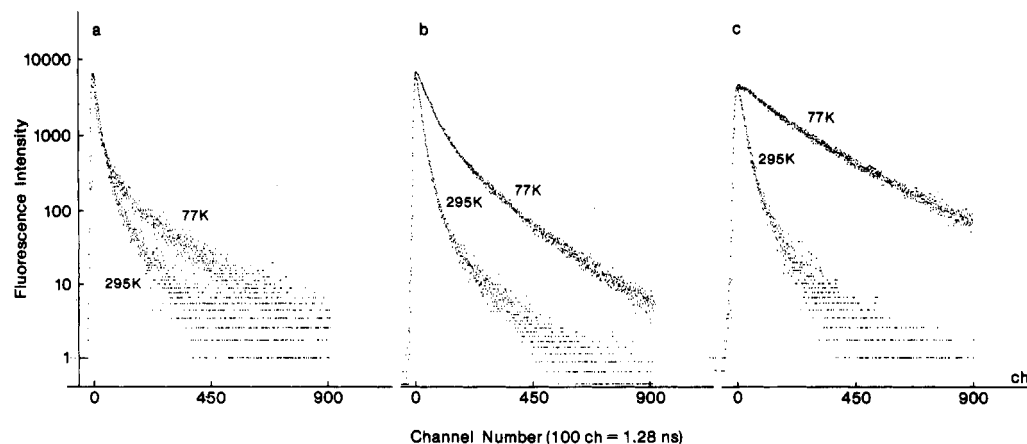
Channel Number (100 ch = 1.28 ns)

Figure 7. Dependence of the fluorescence decays on the observation wavelength of a RhB monolayer adsorbed on glass at 295 and 77 K: 573 nm (a), 590 nm (b), and 620 nm (c). λ_{ex} = 550 nm. Note that there is no rise observed at 620 nm.[61]

much too large to be attributed to either two- or three-dimensional dimers (1000–1200 cm^{-1}). We take this crude model consideration as a further hint for the presence of higher aggregates ($N > 2$) at lower temperature: three to four molecules aligned in a fluorescent geometry (see (4) in Figure 1) could suffice to generate the red shifts observed at 77 K.[44]

2. *Fluorescence Dynamics. a. Monolayer Systems.* Figure 7 shows the dependence of the observed fluorescence decay on the observation wavelength of a monolayer of RhB at 295 and 77 K. The fluorescence decay at all three wavelengths of 573, 590, and 620 nm at 295 K is dominated by an exponential decay with lifetime $\tau \approx 120$ ps, whose contribution is largest at 590 nm (75%). We believe that this decay is caused by a dimer species D$_{595}$ with fluorescence maximum at 595 nm (see Figure 4, top). The "long tail" observed at 573 and 590 nm can be interpreted as quenched monomer fluorescence, e.g., the decay at 590 nm can be analyzed as a sum of an exponential and a nonexponential component:[1,46] $I(t) = 0.75 \exp(-t/120 \text{ ps}) + 0.25 \exp(-t/3.8 \text{ ns} - 1.33\gamma(t/3.8 \text{ ns})^{1/3})$ with $\gamma = 2.5$. The first term represents the exponential fluorescence decay of the dimer and the second the monomer fluorescence ($\tau_f = 3.8$ ns^{47}) quenched by dimer or aggregate species, according to the two-dimensional Förster-type energy transfer.[1,2] The long tail observed at 620 nm, which is more intense than that at 573 and 590 nm, can be thought of as being comprised of quenched monomer fluorescence and of an additional contribution from a second dimer species, emitting at longer wavelengths (see shoulder at 640 nm in Figure 4 (top) and especially Figure 2). Phosphorescence, in comparison, appears at 690 nm.[4]

Upon cooling to 77 K, a drastic change in the fluorescence decay occurs at all three wavelengths and the decays observed at these

three wavelengths now strongly differ from one another (Figure 7). The decay which is observed at 573 nm is nonexponential and faster than the exponential one at 295 K, whereas the decays at longer wavelengths are clearly slower. A look at the fluorescence spectra of Figure 4 (above) shows us that most of the dimers D$_{595}$ are replaced by dimers D$_{623}$ and that at 573 nm the monomer peak becomes visible at 77 K. Thus, the decay at 573 nm is now determined by the fluorescence of the monomer, which is strongly quenched as seen in Figure 7. The decay at 573 nm can be analyzed as almost pure nonexponential Förster-type energy transfer: $I(t) = 0.02 \exp(-t/2.5 \text{ ns}) + 0.98 \exp(-t/3.8 \text{ ns} - 1.33\gamma(t/3.8 \text{ ns})^{1/3})$ with $\gamma = 4.5$. At 590 nm, there is a large additional contribution from a long-lived component (3.8 ns). This long-lived component dominates the decay at 620 nm. The slight nonexponential decay at 620 nm could be explained with the emission of several species and/or with an enhanced decay due to dimer–dimer migration (see section IV2d).

The observed change of the fluorescence dynamics at 77 K strongly supports the idea of a structural rearrangement. The analysis of the decays at 295 and 77 K together with the fluorescence and absorption spectra at 295 and 77 K lead to the following picture: there are at least two emitting species present at 295 K, monomer M$_{575}$, dimer D$_{595}$, and perhaps another dimer or aggregate emitting at longer wavelengths. Upon cooling to 77 K, many of the D$_{595}$ dimers with short lifetime (120 ps) are transformed into an aggregate species D$_{623}$ with longer fluorescence lifetime (3.8 ns). The increased fluorescence lifetime explains the drastic increase of fluorescence intensity at 77 K.

b. *Multilayer Systems.* The dependence of the fluorescence decay on the observation wavelength of a 50-Å evaporated film (about four molecular layers) is qualitatively analogous to the case of the monolayer system. The main differences are the shorter lifetime of the fast exponential decay of about 45 ps and the smaller contribution of species with long lifetime (only about 1/5 of the monolayer system) observed at 630 nm and 77 K.

c. *Lifetimes.* McRae and Kasha's theory[17] gives an expression for the dependence of the radiative rate constant of dimers k_r^D on the angle of the monomer transition moments (for in-plane nonparallel transition moments) as $k_r^D = k_r^M \cos^2 \theta$, e.g. for perfectly parallel ($\theta = 90°$) transition moments, the radiative rate constant is zero and for the head-to-tail geometry ($\theta = 0°$), it corresponds to the radiative lifetime of the monomer k_r^M (see Figure 1). Taking the twisted sandwich-like geometry of solution dimers with its angle between the transition moments of 30° [20] one should expect a radiative lifetime of 63 ns ($k_r^M = 1/4.25$ ns^{48}). Actually found was a fluorescence lifetime of 38 ns^4 for isolated

(44) It should be mentioned here that our dimer models assume flat, isotropically^{45} adsorbed monomers, which arrange in the plane according to their mutually exerted forces (mainly electrostatic in nature) at higher coverages. Heinz et al.,[12] however, suggested an angle of about 56° of the long molecule axis (Rh6G, Rh101) with the surface, as it would arise from adsorption via one amino group and the carboxylphenyl group. This geometry would allow a denser packing of molecules in the monolayer and result in a larger splitting. Since their technique of sample preparation differs from ours, a comparison may not be straightforward, however.

(45) Nickel, B. *Ber. Bunsenges. Phys. Chem.* **1971**, *75*, 795.

(46) An identical decay law, comprised of an exponential with nonexponential Förster contribution observed by us,[1] was also found by Anfinrud et al. (Anfinrud, P.; Crackel, R. L.; Struve, W. S. *J. Phys. Chem.* **1984**, *88*, 5873) for various submonolayer systems of cresyl violet adsorbed on quartz. The latter paper showed in detailed analyses that fits with the above mechanism yielded nearly statistical autocorrelations and that these fits could clearly be distinguished from biexponential decays. Furthermore, our decays are dominated by a fast component whose lifetime is about 30 times shorter than that of the slow component. Complications, as found by Ware et al. (James, D. R.; Ware, W. R. *Chem. Phys. Lett.* **1985**, *120*, 455; James, D. R.; Lin, Y.-S.; de Mayo, P.; Ware, W. R. *Chem. Phys. Lett.* **1985**, *120*, 460.) for the analyses of biexponential decays with similar lifetimes should be absent in our systems, therefore.

(47) The fluorescence lifetime of adsorbed monomer species^{1,15} is longer than that of molecules in solution^2 due to enhanced rigidity.

(48) This value is for the base form of RhB in ethanol.[49] We assume the same radiative lifetime for adsorbed species. This seems to be justified considering the relative independence of the radiative lifetime on the solvent as has been established for the related dye fluorescein.[50]

(49) Sadkowski, P. J.; Fleming, G. R. *Chem. Phys. Lett.* **1978**, *57*, 526.

(50) Martin, M. M. *Chem. Phys. Lett.* **1975**, *35*, 105.

dimers of RhB in a matrix of aqueous 10 M LiCl solution at 77 K. At 295 K, no fluorescence of RhB dimers, even at 0.2 M dye concentration, could be detected, due to the small fluorescence quantum yield and the overlapping of both monomer and dimer fluorescence and absorption spectra. However, transient absorbance measurements revealed a lifetime of 100 ps for RhB dimers in aqueous solution at 295 K.[51] The short lifetime of dimers in solution is explained with a dissociative mechanism which produces a vibrationally hot molecule in addition to a relaxed ground-state monomer. Our fluorescence lifetime of 120 ps for the adsorbed in-plane dimer D_{595} at 295 K is, therefore, tentatively interpreted as the result of a fast "dissociation" reaction. The longer lifetime of about 3.8 ns at 77 K of a monolayer system (Figure 7) could be understood as slowed down dimer dissociation and the very long lifetime of 38 ns in a 77 K matrix could be due to hindered dissociation in the rigid environment.

Whereas dimer formation in solution is mainly due to hydrophobic interaction,[29] these forces would not play a dominant role on a surface (dry system), where dispersion forces and electrostatic interaction of the zwitterion with the polar surface and with other monomer molecules may prevail. Adsorbed molecules perform librational and vibrational motions with respect to the surface, e.g. for benzene adsorbed on Vycor glass and graphite, the frequency range of these vibration is about 30-140 cm^{-1}.[52] In addition, there may also be a translational degree of freedom: for example, acenaphthene adsorbed on SiO_2 moves about 0.1 Å/ns.[53] Also, a vibration of the two monomer moieties with respect to each other should be considered as well as structural changes in the excited monomer itself.[54] In total, there are many parameters which may influence the bond in a dimer adsorbed on a surface. Small distortions during the excited-state lifetime may lead to a "dissociation", which does not necessarily imply a large separation of the monomers from one another.

The situation of a RhB dimer in a multilayer is even more difficult to assess, because of the unknown structure of layers produced by the evaporation technique. The short fluorescence lifetime of about 45 ps for dimers in multilayers could be due to a fast nonradiative decay induced by coupling to the lattice modes, available in a multilayer system, and could also explain the absence of a long-lived component.

d. Polarization. The fluorescence decay curves of both monolayer and multilayer systems showed independence of the decay kinetics on the direction of polarization of the emitted light at 295 and 77 K. The degree of polarization P ($P = (I_{\parallel} - I_{\perp})/(I_{\parallel} + I_{\perp})$, $I_{\parallel}$ and $I_{\perp}$ being the fluorescence intensities parallel and perpendicular to the polarization of the excitation beam[55]), however, strongly depended on temperature. P was almost 0.4 at 295 K, but close to zero at 77 K. The high value of P at 295 K excludes a major contribution of either monomer–monomer or dimer–dimer energy migration to the fast (exponential) fluorescence decay (Figure 7). Formerly, the mechanism of monomer–monomer energy migration had been assigned for this fast decay by Willig et al.[56] Since our monolayer systems turned out to contain more dimeric than monomeric species (Figures 2 and 4), which are both simultaneously excited by λ_{ex} = 550 nm, energy migration should be more probable among the dimer population. Due to the short dimer fluorescence lifetime of about 120 ps, which yields a small γ,[55] depolarization due to dimer–dimer migration does not occur to an appreciable extent, apparently. At 77 K,

however, where most dimer species have a much longer lifetime of about 3.8 ns, almost complete depolarization is observed due to efficient energy migration among dimers. This may explain (in addition to the possibility of several emitting species of long lifetimes) the deviations of the fluorescence decay from an exponential at 77 K (Figure 7).

3. Possible Role of Dimers in Hole Injection. This work implies the existence of fluorescent dimers with a lifetime of about 120 ps adsorbed on glass at ambient temperatures. This may be of considerable importance for the interpretation of electrochemical measurements concerning the hole injection capabilities of dye dimer molecules. From the observed decrease of the photocurrent which occurs when the coverage is increased above a monolayer and from the absence of a pronounced dimer peak at shorter wavelength in the action spectrum, it was generally concluded that dimers are inactive as hole injectors.[22,57]

The present work shows that dimers could indeed be efficient hole injectors, because the decrease of the photocurrent (I_{ph}) can now be alternatively associated with a fast nonradiative decay (k_{non}) (e.g., dissociation) of the dimers instead of a small dimer electron transfer rate (k_e): $I_{ph} \propto \phi_{ct} = k_e/(k_e + k_{non})$.

The action spectra might have been misinterpreted, because authors in the past were looking for a dimer peak as created by blue-shifted nonfluorescent solution dimers.[4] On the surface, however, all types of dimers (nonfluorescent and fluorescent) contribute to the overall absorbance. The sum of a distribution of blue- and red-shifted dimers and of residual monomers makes the absorption spectrum look similar to that of a monomer. The presence of dimeric species might be deduced, however, from the relative intensity of the short wavelength shoulder. The ratio of I(shoulder)/I(maximum) is about 0.3 for solution monomers, but about 0.37–0.49 for a monolayer containing adsorbed dimers (Figures 2 and 5) or even 0.80, as was found in an action spectrum.[57]

The direct proof for the injection by dimers has been obtained by measuring the fluorescence decay of a RhB monolayer adsorbed on a single crystal of anthracene ($\Delta G_0 < 0$, down hill reaction) and by comparing this decay with the decay of a corresponding monolayer adsorbed on phenanthrene ($\Delta G_0 > 0$). The former yields a decay dominated by an exponential decay of about 50 ps[58] whereas the latter gives a decay of about 100 ps,[58] very similar to this work. The rate constant for hole injection of dimers k_h = k_{obsd}(anthracene) – k_{obsd}(phenanthrene) is obtained as 1×10^{10} s^{-1} which is of the same magnitude as the rate constant for electron transfer of RhB monomers. The rate constant for electron transfer of RhB monomers adsorbed on an anthracene single crystal has been obtained by measuring the fluorescence decay of 1/100 monolayer (to avoid energy transfer) and was found to be 9×10^9 s^{-1}.[58]

The quantum efficiency of charge transfer for dimers in our monolayer system is according to above rate constants ϕ_{ct} = $10^{10}/(10^{10} + 10^{10}) \approx 0.5$, which is about half the value obtained for monomers. Hole injection by dimers of RhB adsorbed on TiO_2 and SnO_2 also was deduced by Itoh et al.[15] from electrochemical measurements with equal quantum yields for monomers and dimers, in qualitative agreement with our results. Quantum yields found in the literature for other monolayer systems range from ≤0.03[23] to 0.8.[59] The high value of 0.8 was obtained for preassembled monolayers of long-chain cyanine dyes transferred to the surface of indium oxide, whereas the very low values of 0.03 were observed in monolayers of RhB adsorbed on zinc oxide from solution. There are two frequent explanations found in the literature for the low charge-transfer (CT) quantum yields in monolayers: (a) the CT process itself and (b) competing processes, i.e., reduced CT capability of dimer molecules[57] or fast competitive energy transfer in monolayer systems.[60] We now can add a third

(51) Smirl, A. L.; Clark, J. B.; Van Stryland, E. W.; Russell, B. R. *J. Chem. Phys.* **1982**, *77*, 631.

(52) (a) Ron, A.; Folman, M.; Schnepp, O. *J. Chem. Phys.* **1962**, *36*, 2449. (b) Stockmeyer, R.; Monkenbusch, M. *Vibrations at Surfaces*, Caudano, R., Gilles, J.-M., Lucas, A. A., Ed.; Plenum Press: New York, 1982.

(53) Bauer, R. K.; Borenstein, R.; de Mayo, P.; Okada, K.; Rafalska, M.; Ware, W. R.; Wu, K. C. *J. Am. Chem. Soc.* **1982**, *104*, 4635.

(54) Andreev, R. B.; Bobovich, Ya. S.; Bortkevich, A. V.; Volosov, V. D.; Tsenter, M. Ya. *Opt. Spectrosc.* **1976**, *41*, 462.

(55) (a) Agranovich, V. M.; Galanin, M. D. *Electronic Excitation Energy Transfer in Condensed Matter*; North-Holland: Amsterdam, 1982. (b) Kawski, A. *Z. Naturforsch.* **1963**, *18a*, 961.

(56) Willig, F.; Blumen, A.; Zumofen, G. *Chem. Phys. Lett.* **1984**, *108*, 222.

(57) Killesreiter, H. *Ber. Bunsenges. Phys. Chem.* **1978**, *82*, 503.

(58) Kemnitz, K.; Tamai, N.; Yamazaki, I.; Nakashima, N.; Yoshihara, K., manuscript in preparation.

(59) Arden, W.; Fromherz, P. *Ber. Bunsenges. Phys. Chem.* **1978**, *82*, 868.

(60) Liang, Y.; Ponte Goncalves, A. M.; Negus, D. K. *J. Phys. Chem.* **1983**, *87*, 1.

possibility: fast nonradiative (dissociative) decay of dimers reduces ϕ_{ct}. We believe that monolayer systems of RhB are comprised to a considerable extent of dimeric species (see Figure 2). Therefore, energy transfer in our system is perhaps not the dominant mechanism for deactivation, since there is no suitable acceptor present for the energy transfer from dimers. Assuming that it is really the dissociative mechanism which determines the short dimer lifetime, it should be possible to increase ϕ_{ct} by preventing the dimers from dissociating. This may be realized for RhB dimers at 77 K in a rigid matrix (τ_f = 38 ns[4]) or for cyanine dimers in highly organized monolayers of long-chain dye molecules.[59]

---

(61) From the absence of a rise at longer wavelengths, we exclude the possibility of multistep migration or energy transfer from originally excited monomeric or dimeric RhB species to impurity molecules (which might be present in a concentration of 1 in 100, see Experimental Section) which in turn might fluoresce at longer wavelengths. It appears that the species which fluoresce at 620 nm are directly excited and have to be identified as RhB aggregates.

V. Summary

The main goal of this paper was to point to the existence of fluorescent short-lived RhB dimers in the adsorbed state at ambient temperature. For this purpose, we reported the temperature- and wavelength-dependent fluorescence decays of various RhB assemblies as well as their temperature-dependent fluorescence and absorption spectra. We also discussed the sensitization capability and quantum efficiency of RhB dimers. The latter might be improved if it were possible to reduce the fast nonradiative decay channels of excited RhB dimers.

Registry No. Rhodamine B, 81-88-9; quartz, 14808-60-7.

Avoided Scattering along the Relative Velocity Vector: Importance for Crossed Molecular Beam Experiments Involving Long-Lived Collision Complexes

Kjell Rynefors,* Leif Holmlid, and Per Anders Elofson

Department of Physical Chemistry GU, University of Göteborg and Chalmers University of Technology, S-412 96 Göteborg, Sweden (Received: February 25, 1986)

The separability of center-of-mass scattering intensity $I_{cm}(\vartheta,u)$ for long-lived complexes, which is often implied in the interpretation of crossed molecular beam results, has been investigated. Our previously published statistical algorithm of the RRKM type has been applied to the reactions K + RbCl and O(^{1}D) + H$_2$. Product angular momenta and the final velocity u were found to vary strongly with the center-of-mass scattering angle ϑ. This provides evidence for a coupling between u and ϑ. Due to selection and projection effects this coupling is more pronounced in the laboratory than in the center-of-mass coordinate space. It was also found that scattering is avoided along the relative velocity vector in laboratory space for a wide range of conditions. The implications for crossed molecular beam experiments are discussed.

1. Introduction

Crossed molecular beam experiments have become increasingly important to the study of elementary reactions ever since Taylor and Datz completed their study on the system K + HBr.[1] The importance of the conservation of total angular momentum for the angular distributions of scattering intensity in such experiments has by now been recognized for a long time.[2-4] The effects of angular momentum conservation were first described by Herschbach[5] for long-lived complexes in a fashion similar to the theory of nuclear reactions. In the case of a collision between an atom and a diatomic molecule, the distribution of scattered product atoms can be described by the angle ϑ between reactant and product relative velocity g. If a long-lived collision complex is formed, the memory of the initial direction of the reactants is lost and all product scattering directions appear to be of equal probability. In the limital case where orbital angular momentum dominates and is approximately conserved, the product scattering in an infinitesimally thin plane defined by the incoming beams was shown to follow a $1/(\sin \vartheta)$ distribution.[5] For most systems

the scattering is somewhat modified by the influence of the rotational angular momenta. Results of this type are important in many crossed molecular beam experiments and the $1/(\sin \vartheta)$ distribution gives rise to forward and backward peaks in the laboratory (lab) angular distributions.

An approximate form of the center-of-mass (cm) scattering in the beam plane was proposed by Herschbach et al.[6] The dependence on ϑ and velocity u of the product molecule was assumed to be separable

$$I_{cm}(\vartheta,u) = T(\vartheta) \ U(u) \qquad (1)$$

$T(\vartheta)$ was given as

$$T(\vartheta) = \sin \vartheta^*/\sin \vartheta \qquad \text{for } \vartheta^* \le \vartheta \le 180 - \vartheta^*$$

$$T(\vartheta) = 1 \qquad \text{for } \vartheta < \vartheta^* \text{ and } \vartheta > 180 - \vartheta^* \qquad (2)$$

where the adjustable parameter ϑ^* was included to take into account the effects of rotational angular momentum in the reactant and product channels. This functional form has later been applied to several experiments, e.g., ref 7 and 8. A modified form by Entemann has also been used.[9-11] In all these cases, the energy

---

(1) Taylor, E. H.; Datz, S. *J. Chem. Phys.* **1955**, *23*, 1711-1718.
(2) Levine, R. D.; Bernstein, R. B. *Molecular Reaction Dynamics*; Oxford University Press: Oxford, 1974.
(3) Toennies, J. P. In *Physical Chemistry*; Eyring, H., Henderson, D., Jost, W., Eds.; Academic: New York, 1974; Vol. VIA.
(4) Smith, I. W. M. *Kinetics and Dynamics of Elementary Gas Reactions*; Butterworths, London, 1980.
(5) Herschbach, D. R. *Discuss. Faraday Soc.* **1962**, *33*, 149-161.

(6) Miller, W. B.; Safron, S. A.; Herschbach, D. R. *Discuss. Faraday Soc.* **1967**, *44*, 108-122.
(7) Aniansson, G.; Creaser, R. P.; Held, W. D.; Holmlid, L.; Toennies, J. P. *J. Chem. Phys.* **1974**, *61*, 5381-5388.
(8) Stolte, S.; Proctor, A. E.; Bernstein, R. B. *J. Chem. Phys.* **1976**, *65*, 4990-5008.